products, and their environment; λ represents the vertical separation between the product and reactant potential energy surfaces.

Expression A is only valid when the series of reactions under study is homogeneous, i.e., when λ and the electronic coupling factors k_E are invariant throughout the series. One important consideration in respect to the electronic factors is whether the intersite distance and conformation are constant throughout the three systems we have studied. We intend to examine this closely by energy-minimized modeling, nonradiative electronic transfer, and two-dimensional NMR experiments. However, for the moment we rely only on the surmise that the configuration of the complex is primarily set by the electrostatic interactions between the cationic lysines of the protein and the anionic groups on the uroporphyrin periphery and that differences in electron density at the metal centers are insignificant in governing the transfer distance. Such differences in electron density arise from the electron-transfer act itself and from substitution of different metals in the heme and uroporphyrin moieties. In this assumption we follow those who have investigated electron transfer in protein–protein associated systems[15-22] and those who covalently link transition-metal complexes to protein surface sites.[8-14]

On the strength, or weakness, of these assumptions we point out that λ = 0.81 V from our data is in line with the values estimated by McLendon and Miller[18] and by Conklin and McLendon[19] in their work on protein–protein complexes and by Meade, Gray, and Winkler[14] for the systems involving ruthenium modifications to cytochrome *c*. To date, all such reactions involving electron transfer into, or out of, a heme (or modified heme) protein show λ values near 1 eV.

In conclusion, we note that by adjusting the ionic strength in aqueous systems containing cytochrome *c* and a highly anionic porphyrin, such as uroporphyrin or its metallo derivatives, we can switch from a diffusional, bimolecular photoinduced electron-transfer process to one that occurs unimolecularly within a preformed electrostatically bound protein–porphyrin complex. In this we differ from Cho et al.[23] who reported only a diffusional type with related systems. Our system on the one hand is reminiscent of protein–protein self-associated complexes because the association of the units relies on electrostatic docking forces. On the other hand it resembles the covalently linked protein–Ru complex systems where one member of the couple is a small molecule located at the protein surface. As in these approaches, our system removes complications that result from diffusion. Perhaps the uroporphyrin/cytochrome *c* system offers an experimentally simpler approach. Further work on extending and refining Figure 10 is in progress.

Acknowledgment. This research has been supported in part by NIH Grant GM31603 and by the Center for Photochemical Sciences at Bowling Green State University. We are grateful to Professors F. Scandola and V. Balzani for useful discussions. We express our thanks particularly to Dr. W. E. Ford for his very useful help during the early stages of this project.

Registry No. Uroporphyrin, 26316-36-9.

Hydrazines: New Charge-Transfer Physical Quenchers of Singlet Oxygen

E. L. Clennan,* L. J. Noe,* E. Szneler, and T. Wen

Contribution from the Department of Chemistry, University of Wyoming, Laramie, Wyoming 82070. *Received December 14, 1989*

Abstract: The rates of reaction of singlet oxygen with 25 hydrazines were determined by following the emission of singlet oxygen at 1270 nm as a function of time. These data are utilized to discuss various options for the quenching mechanism including electron transfer, electronic to vibrational energy transfer, and a contact charge-transfer process.

It is now well established that singlet oxygen is responsible for photodynamic destruction of both biologically and commercially important molecules. As a consequence, it is of some practical importance to search for and to investigate the properties of molecules capable of physically quenching[1] this reactive species. Molecules that have been identified as physical quenchers of singlet oxygen include amines,[2] sulfides,[3] carotenoids,[4] metal chelates,[1b] nitroxides,[1b] phenols,[1b] inorganic anions,[1b] and nitroso compounds.[1b]

It has been recognized that physical quenching of $^1O_2$ occurs by four distinctly different mechanisms:[1a] (an energy-transfer mechanism (for example, carotenoids have low-lying excited states capable of accepting the energy from the $^1\Delta_g$ state of O_2); (2) a reactive quenching mechanism that involves covalent bonding of $^1O_2$ to a substrate followed by decomposition to triplet oxygen

Chart I

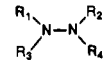

1. $R_1 = R_2 = R_3 = R_4 = Me$
2. $R_1 = R_2 = R_3 = R_4 = iBu$
3. $R_1 = R_2 = Me$; $R_3 = R_4 = Et$
4. $R_1 = R_2 = Me$; $R_3 = R_4 = nPr$
5. $R_1 = R_2 = Me$; $R_3 = R_4 = nBu$
6. $R_1 = R_2 = Me$; $R_3 = R_4 = nPe$
7. $R_1 = R_2 = Me$; $R_3 = R_4 = iBu$
8. $R_1 = R_2 = Me$; $R_3 = R_4 = neoPe$
9. $R_1 = R_2 = R_3 = Me$; $R_4 = iBu$
10. $R_1 = R_2 = R_3 = Me$; $R_4 = neoPe$
11. $R_1 = R_3 = Me$; $R_2 = R_4 = iBu$
12. $R_1 = R_3 = Me$; $R_2 = R_4 = neoPe$
13. $R_1 = R_2 = R_3 = R_4 = CD_3$

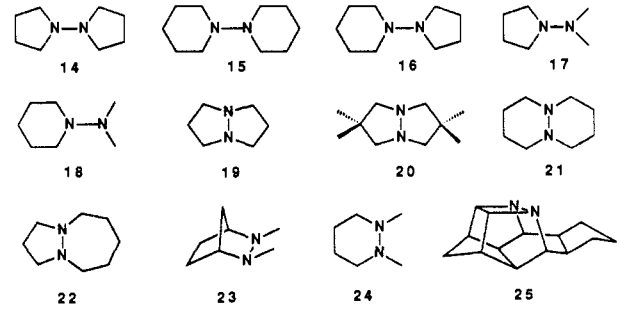

(1) (a) Foote, C. S. In *Singlet Oxygen*; Wasserman, H. H., Murray, R. W., Eds.; Academic Press: New York, 1979; p 139. (b) Bellus, D. In *Advances in Photochemistry*; Pitts, J. N., Hammond, G. S., Gollnick, K., Eds.; John Wiley and Sons: New York, 1979; Vol. 11, p 105.

(2) (a) Ouannes, C.; Wilson, T. *J. Am. Chem. Soc.* **1968**, *90*, 6527. (b) Ogryzlo, E. A.; Tang, C. W. *J. Am. Chem. Soc.* **1970**, *92*, 5034. (c) Young, R. H.; Martin, R. L. *J. Am. Chem. Soc.* **1972**, *94*, 5183. (d) Smith, W. F., Jr. *J. Am. Chem. Soc.* **1972**, *94*, 186. (e) Young, R. H.; Martin, R. L.; Feriozi, D.; Brewer, D.; Kayser, R. *Photochem. Photobiol.* **1973**, *17*, 233. (f) Monroe, B. M. *J. Phys. Chem.* **1977**, *81*, 1861. (g) Saito, I.; Matsuura, T.; Inoue, K. *J. Am. Chem. Soc.* **1981**, *103*, 188. (h) Manring, L. E.; Foote, C. S. *J. Phys. Chem.* **1982**, *86*, 1257. (i) Saito, I.; Matsuura, T.; Inoue, K. *J. Am. Chem. Soc.* **1983**, *105*, 3200.

(3) (a) Jensen, F.; Foote, C. S. *J. Am. Chem. Soc.* **1987**, *109*, 1478. (b) Nahm, K.; Foote, C. S. *J. Am. Chem. Soc.* **1989**, *111*, 1909. (c) Ando, W.; Takata, T. In *Singlet Oxygen*; Reaction Modes and Products. Part 2; Frimer, A. A., Ed.; CRC Press: Boca Raton, 1985; Vol. III, p 1.

(4) (a) Foote, C. S.; Denny, R. W. *J. Am. Chem. Soc.* **1968**, *90*, 6233. (b) Foote, C. S.; Chang, Y. C.; Denny, R. W. *J. Am. Chem. Soc.* **1970**, *92*, 5216.

0002-7863/90/1512-5080$02.50/0

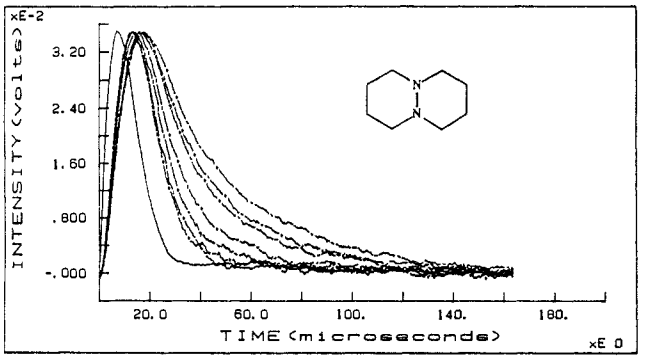

Figure 1. Normalized $^1O_2$ phosphorescence decay curves in the absence and presence of increasing amounts of hydrazine. The detector response is also shown as a sharp peak with a displaced maximum. The data were extracted with use of the previously described numerical deconvolutional analysis.

and substrate (this mechanism has been invoked to explain quenching by dialkyl sulfides); (3) an electronic to vibrational energy transfer that has been shown to limit the lifetime of $^1O_2$ in condensed media;[5] and (4) a charge-transfer mechanism that has been invoked to explain the observation of a correlation between ease of ionization of amines in the gas phase[1b] and their quenching ability.

The study of the quenching of $^1O_2$ by amines in solution, in contrast to their study in the gas phase, has been hampered by the inaccessibility of thermodynamically significant oxidation potentials. As a result, the driving force ($\Delta G°$) for a hypothetical electron-transfer-quenching process promoted by the ability of the solvent to stabilize ion pairs is unavailable.

This inability to quantitatively study the quenching of $^1O_2$ by easily ionizable nitrogen compounds can be circumvented to a degree by studying the homologues of the amines, the hydrazines. Hydrazine radical cations prefer an olefin-like geometry allowing both charge and spin to be shared by the two nitrogens, and as a result they are more stable than amine radical cations.[6] Hydrazines, when structurally allowed, prefer to exist in 90° conformations[7] in order to minimize destabilizing lone-pair lone-pair interactions and can be reversibly or quasireversibly oxidized to their cations.

We report here the physical quenching rates of $^1O_2$ by 25 hydrazines (Chart I). These data are utilized to discuss various options for the quenching mechanism, including electron transfer.

Results

The singlet oxygen quenching rates were determined by monitoring the hydrazine-induced deactivation of $^1O_2$. The concentration of singlet oxygen as a function of time was measured by using the previously described[8] laser based kinetic apparatus.

Data for the [4.4.0] hydrazine **21** in benzene are shown in Figure 1 with acridine (λ_{irr} = 355 nm) as sensitizer. The decay curves with decreasing lifetimes represent solutions with increasing concentrations of **21**. The rate of deactivation of singlet oxygen by **21** was extracted by using eqs 1 and 2. The rate constants k_d, k_S, and k_H represent the solvent, sensitizer, and hydrazine-induced deactivation of singlet oxygen. Rate constants k_S and k_H are the sum of the chemical (k_r) and physical (k_q) rates of removal of singlet oxygen by the sensitizer and hydrazine, respectively.

$$-d[^1O_2]/dt = k_{obsd}[^1O_2] \quad (1)$$

$$k_{obsd} = k_d + k_H[\text{hydrazine}] + k_S[S] \quad (2)$$

Table I. Hydrazine Oxidation Potentials and Singlet Oxygen Quenching Rates[a,b]

H[c]	$E°'$	10^7k (M^{-1} s^{-1})	H[c]	$E°'$	10^7k (M^{-1} s^{-1})
1	0.33 (2.64)	18.6	**14**	0.02 (-4.51)	34.6
2	0.37 (3.56)	0.0298	**15**	0.40 (4.25)	2.76
3	0.31 (2.17)	6.76	**16**	0.20 (-0.36)	26.1
4	0.31 (2.17)	4.40	**17**	0.17 (-1.05)	55.8
5	0.30 (1.94)	3.90	**18**	0.36 (3.33)	15.5
6	0.31 (2.17)	4.71	**19**	0.08 (-3.13)	76.8
7	0.33 (2.64)	1.29	**20**	-0.01 (-5.21)	131
8	0.32 (2.40)	0.525	**21**	0.28 (1.48)	28.9
9	0.33 (2.64)	9.57	**22**	0.01 (-4.74)	71.2
10	0.34 (2.87)	10.5	**23**	0.20 (-0.36)	54.8
11	0.34 (2.87)	2.18	**24**	0.23 (-0.36)	46.2
12	0.34 (2.87)	0.130	**25**	0.81 (13.7)	27.6
13		18.6			

[a] Oxidation potentials are reported in volts versus SCE. [b] Corresponding free energies in kcal/mol are in parentheses. [c] Hydrazine.

Table II. Solvent Effects on Singlet Oxygen Quenching Rates

hydrazine	solvent	$10^{-7}k$ (M^{-1} s^{-1})
1	benzene	18.0
	$(CH_3)_2CHOH$	2.14
	CF_3CH_2OH	0.115
5	benzene	3.90
6	benzene	0.932
7	benzene	0.592
9	benzene	6.78
14	benzene	72.2
	$(CH_3)_2CHOH$	17.5
	CF_3CH_2OH	0.216
15	benzene	1.70
	$(CH_3)_2CHOH$	0.3197
	CF_3CH_2OH	0.0236
20	benzene	178.0
21	benzene	27.8
	$(CH_3)_2CHOH$	7.42
	CF_3CH_2OH	0.254

Irradiation of an acetone-d_6 NMR sample containing equal amounts of triethylamine, tetramethylhydrazine **1**, and 2×10^{-5} M Rose Bengal as a sensitizer demonstrated after several hours triethylamine had been totally consumed and no decomposition of **1** could be detected. Since **1** and triethylamine remove singlet oxygen from solution at about the same rate,[9] this indicates that the k_r contribution to k_H for **1** is very small and that k_H and k_q are approximately equal. We have no evidence that this is not also the case for the other hydrazines examined, and we would be surprised if k_r were not minimal in comparison to k_q for all 25 hydrazines.

The quenching rates, in CH_3CN, for hydrazine **21** and the other 24 hydrazines are listed in Table I. Each rate constant represents the average of at least two independent determinations. The reproducibility for multiple determinations was ±15% and in many cases less than ±10%. The driving force ($\Delta G°$) in kcal/mol for each reaction is also reported in Table I and was calculated by using eq 3.[10] The variables $E°'$(hydrazine), $e^2/\epsilon a$, and ΔE_{oo} represent the oxidation potential of the hydrazine, the reduction

$$\Delta G° = 23.06[E°'(\text{hydrazine}) - E°'(O_2/O_2^{\bullet-}) - e^2/\epsilon a] - \Delta E_{oo} \quad (3)$$

potential of triplet oxygen (-0.82 V in CH_3CN),[11] the enthalpy change as a result of bringing two ions to encounter distance a in a solvent of dielectric constant ϵ (0.06 eV in CH_3CN),[11] and the vibrationless $^1\Delta_g$ O_2 excitation energy (22.5 kcal/mol),[12] respectively.

(5) (a) Ogilby, P. R.; Foote, C. S. *J. Am. Chem. Soc.* **1983**, *105*, 3423. (b) Rodgers, M. A. *J. Am. Chem. Soc.* **1983**, *105*, 6201. (c) Hurst, J. R.; Schuster, G. B. *J. Am. Chem. Soc.* **1983**, *105*, 5756. (d) Schmidt, R.; Brauer, H.-D. *J. Am. Chem. Soc.* **1987**, *109*, 6976.
(6) Nelsen, S. F.; Peacock, V.; Weisman, G. R. *J. Am. Chem. Soc.* **1976**, *98*, 5269.
(7) Nelsen, S. F. *Acc. Chem. Res.* **1981**, *14*, 131.
(8) Clennan, E. L.; Noe, L. J.; Wen, T.; Szneler, E. *J. Org. Chem.* **1989**, *54*, 3581.
(9) Wilkinson, F.; Brummer, J. G. *J. Phys. Chem. Ref. D* **1981**, *10*, 809.
(10) Rehm, D.; Weller, A. *Isr. J. Chem.* **1970**, *8*, 259.
(11) Peover, M. E.; White, B. S. *Electrochim. Acta* **1966**, *11*, 1061.
(12) Frimer, A. A. *The Chemistry of Functional Groups, Peroxides*: John Wiley and Sons: New York, 1983; Chapter 7, p 201.

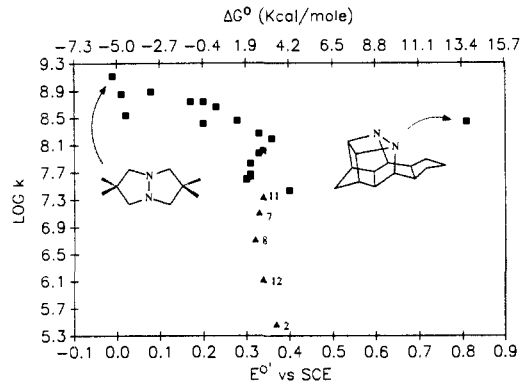

Figure 2. A plot of the log of the quenching rates (Table I) versus the oxidation potential and free energy of the hypothetical singlet oxygen–hydrazine electron-transfer reaction.

Scheme I

$$\text{hydrazine} + {}^1O_2 \underset{k_{-d}}{\overset{k_d}{\rightleftharpoons}} (\text{hydrazine}\cdots{}^1O_2)$$

$$(\text{hydrazine}\cdots{}^1O_2) \xrightarrow{k_{et}} \text{hydrazine}^{\bullet+} + O_2^{\bullet-}$$

The oxidation potentials of **2**, **9**, **10**, and **12** were determined by cyclic voltammetry and exhibit chemically reversible and electrochemically quasireversible behavior typical of hydrazines. The oxidation potentials of the remaining hydrazines are those reported by Nelsen and co-workers.[13]

Additionally, the quenching rates for nine of the hydrazines were determined in benzene and four in 2-propanol and 1,1,1-trifluoroethanol. These data are presented in Table II.

Discussion

In order to determine the feasibility of an electron-transfer mechanism for these new quenching reactions a plot of log k_{obs} versus the oxidation potentials of the hydrazines and driving force, $\Delta G°$, for the reactions was constructed and is depicted in Figure 2. The rates span a range of almost four orders of magnitude from 1.3×10^9 to 3.0×10^5 M^{-1} s^{-1}, and a dramatic steric effect is observed for the acylic hydrazines with oxidation potentials between 0.3 and 0.4 V versus SCE. The five slowest reacting hydrazines **2**, **7**, **8**, **11**, and **12** are the compounds substituted with at least two β-branched alkyl groups. These compounds span over 50% of the observed log (k) range. These steric interactions are reminiscent of the steric effects observed by Kochi[14] in the study of the reactions of tetraalkyltins with tetracyanoethylene and are indicative of an inner-sphere process. The inner-sphere nature of these quenching reactions is further corroborated by the classical

$$k_{obs} = \frac{k_d}{1 + [k_d/(K_d Z)] \exp([\lambda/4\{1 + \Delta G°'/\lambda\}^2]/RT)} \quad (4)$$

Marcus plot illustrated in Figure 3. The plot was calculated using the logarithmic form of Eqn. 4 which is derived using the steady state approximation for the quenching mechanism shown in Scheme I and inserting the Marcus expression (eq 5) for k_{et}.[15] The anomolously high quenching rate of **25**, despite its high oxidation potential, is most likely due to the unusual carbon framework that ties the alkyl groups back allowing easy access by $^1O_2$.

$$\Delta G_{et}^{\neq} = \frac{\lambda}{4}\left(1 + \frac{\Delta G°'}{\lambda}\right)^2 \quad (5)$$

The Marcus reorganization energy, λ, is the activation barrier for the energetically inaccessible vertical electron transfer reaction

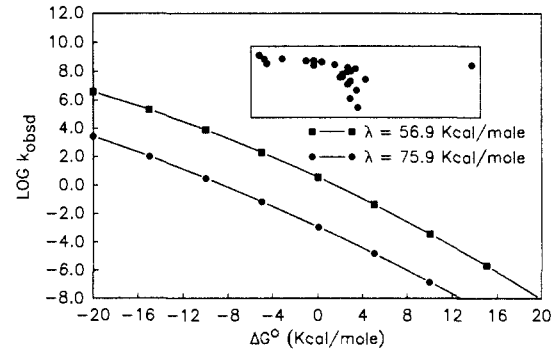

Figure 3. A Marcus free energy plot of the theoretical data juxtaposed with the experimental data for the hydrazines in the box in the upper right hand corner.

that occurs without a geometry change in either the donor or acceptor. The reorganization energy, λ, is numerically four times the free energy of activation for electron transfer and is a result of the constraints of the parabolic Marcus energy surface when $\Delta G° = 0$. The magnitude of the reorganization energy is the result of contributions from both internal geometry changes, λ_i, and resolvation demands, λ_o, in the transition state for electron transfer. Nelsen[16] and co-workers have demonstrated for two hydrazines that λ_o is only a minor component of the hydrazine self-exchange reorganization energy (eq 6). As a result, the reorganization energy, λ, for a hetero electron exchange reaction can be estimated by taking the average of the reorganization energies of the corresponding self-exchange reactions 6 and 7.[17]

$$[R_2N{-}NR_2]_I + [R_2\overset{+}{N}{-}\overset{+}{N}R_2]_{II} \rightleftharpoons [R_2\overset{+}{N}{-}\overset{+}{N}R_2]_I + [R_2N{-}NR_2]_{II} \quad (6)$$

$$[{}^1O_2]_I + [O_2^{\bullet-}]_{II} \rightleftharpoons [O_2^{\bullet-}]_I + [{}^1O_2]_{II} \quad (7)$$

Unfortunately, the free energy of self-exchange electron transfer has not been reported for the hydrazines used in this study. Experimentally determined values for only two hydrazines, **26**

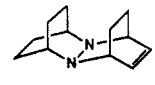

26

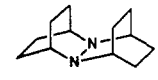

27

(11.77 kcal/mol) and **27** (13.42 kcal/mol), have been reported by Nelsen and co-workers[18] using a NMR line-broadening technique. The success of the Nelsen study with these hydrazines was a direct result of the limited geometry changes allowed by the hydrocarbon skeletons. The hydrazines depicted in Chart I do not have the special geometrical constraints necessary to minimize the internal reorganization that occurs upon oxidation, and as a result the self-exchange electron-transer rates are too slow to be measured by NMR line broadening.

Approximate λ values for many hydrazines, as previously pointed out, can be estimated by realizing that λ is the energy difference between starting materials and products in the vertical self-exchange reaction that occurs without a geometry change in either the reduced or oxidized reactants. This is expressed chemically and mathematically in eq 8a,b where $E(H_H)$ is the

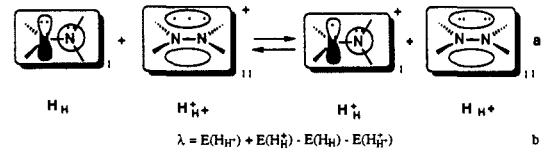

(8)

energy of hydrazine in its stable geometry, $E(H_{H}^{+\bullet})$ is the energy of the hydrazinium ion in its relaxed ground-state geometry,

(13) Nelsen, S. F.; Rumack, D. T.; Meot-Ner, M. *J. Am. Chem. Soc.* **1988**, *110*, 7945.
(14) Fukuzumi, S.; Wong, C. L.; Kochi, J. K. *J. Am. Chem. Soc.* **1980**, *102*, 2928.
(15) A diffusion rate of 2×10^{10} M^{-1} s^{-1}, $Z = 6 \times 10^{11}$ s^{-1}, and $K_d = 0.16$ M^{-1} were used in the calculation.
(16) Nelsen, S. F.; Kim, Y.; Blackstock, S. C. *J. Am. Chem. Soc.* **1989**, *111*, 2045.
(17) Eberson, L. In *Electron Transfer Reactions in Organic Chemistry*; Springer-Verlag: Berlin Heidelberg, 1987.
(18) Nelsen, S. F.; Blackstock, S. C.; Kim, Y. *J. Am. Chem. Soc.* **1987**, *109*, 677.

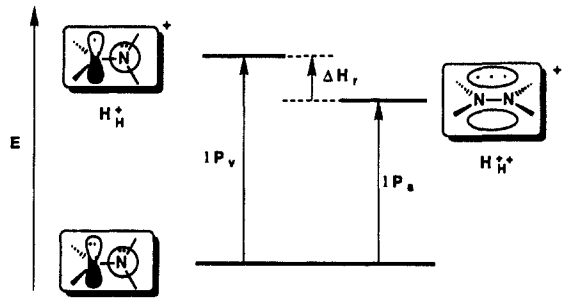

Figure 4. The relationship between gas-phase ionization potentials.

Table III. Force Constants, Vibrational Frequencies, and Bond Lengths for Oxygen Species[a]

molecule	r (Å)[b]	ν (cm^{-1})	k (dyn/cm^{-1})
$^3O_2$	1.207	1580.4	11.77×10^5
O_2	1.330	1097	5.22×10^7
$O_2(^1\Delta_g)$	1.216	1509	10.73×10^5[c]

[a] Values for triplet oxygen and superoxide are from ref 21. [b] The bond length and vibrational frequency for singlet oxygen are from ref 21. [c] Calculated from $[\nu(^1O_2)/\nu(^3O_2)] = [k(^1O_2)/k(^3O_2)]^{1/2}$.

$E(H_{H^+})$ is the energy of the product hydrazine in a distorted geometry corresponding to the ground state of the cationic hydrazinium ion, and $E(H_H^+)$ is the energy of the product hydrazinium ion in a distorted geometry corresponding to the ground-state hydrazine. The enthalpy portion of the quantity $E(H_H^+) - E(H_{H^+})$ is the relaxation energy of the hydrazinium ion (ΔH_r). The relaxation energies of several hydrazines have been experimentally obtained by Nelsen and co-workers[19] from the differences between the vertical and adiabatic ionization potentials of several hydrazines (Figure 4). These enthalpies of relaxation, in the gas phase, cover a remarkably wide range from 18.9 to 38.3 kcal/mol. The remaining value in eq 8b needed to calculate the reorganization energy, λ, is the relaxation energy of the hydrazine, $E(H_{H^+}) - E(H_H)$, which is at present experimentally inaccessible. However, Nelsen demonstrated with AM1 calculations that it is approximately equal to the relaxation energy of the hydrazinium ion. This wide range of relaxation energies is consistent with the very different amounts of internal reorganization required for the various hydrazines to reach the hydrazinium geometry. As a consequence, one unique reorganization energy is simply inadequate to describe the kinetic behavior of all 25 hydrazines. The Marcus curves in Figure 3 were calculated with a lower limit of 38 and an upper limit of 76 kcal/mol for the hydrazine self-exchange reorganization energy.

The activation barrier for the singlet-oxygen self-exchange electron-transfer reaction (eq 7) has also not been measured experimentally. Fortunately, for diatomic singlet oxygen, it can be evaluated conveniently with the vibrational coordinate analysis depicted in eq 9.[20] Using the bond lengths and force constants

$$\lambda_i = \frac{k(^1O_2)k(O_2^{\bullet-})}{k(^1O_2) + k(O_2^{\bullet-})}[r(^1O_2) - r(O_2^{\bullet-})]^2 \qquad (9)$$

for singlet oxygen and superoxide summarized in Table III[21] results in a calculated value of 6.564 kcal/mol for λ_i. A value of λ_o = 69.24 kcal/mol is obtained from eq 10,[17] where r_1, r_2, η, and D are the radii of singlet oxygen and superoxide, the refractive index,

$$\lambda_0 = e^2[1/2r_1 + 1/2r_2] - 1/(r_1 + r_2)[1/\eta^2 - 1/D] \qquad (10)$$

and the dielectric constant of CH_3CN, respectively. The reorganization energy, $\lambda = \lambda_i + \lambda_o$, obtained from eqs 9 and 10 is substantially larger than the experimentally determined value,[22]

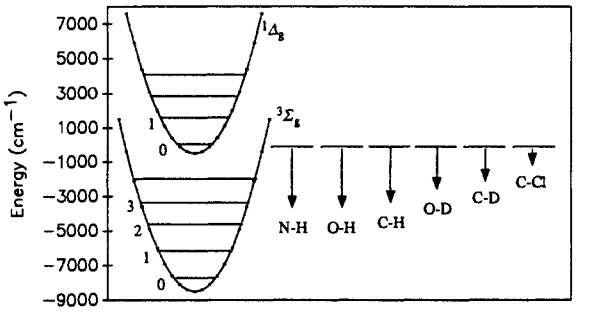

Figure 5. A comparison of the oxygen deactivation energies to solvent oscillator acceptor energies.

in H_2O, of 45.5 ± 0.7 kcal/mol for the triplet oxygen self-exchange reaction. This discrepancy in values probably reflects the more extensive solvation of superoxide in H_2O than in CH_3CN and the resulting larger effective radius for electron transfer.

Corrections for electrostatic interactions (eq 11)[17] in the transition states for electron transfer are only 0.95–1.9 kcal/mol

$$\Delta G^{\circ\prime} = \Delta G^\circ - \frac{331.2}{Dr_{12}} \qquad (11)$$

for hydrazines with radii of 5–10 Å. Consequently, these corrections were not made before adding the free energies for reactions of hydrazines **1–24** to the Marcus plot since they do not change the conclusion that *all of the hydrazines studied react several orders of magnitude faster* (see Figure 3) *than can be accounted for by an electron-transfer process*. An unreasonable reorganization energy of 20 kcal/mol is required to place even the slowest reacting hydrazines within the Marcus region.

A singlet oxygen quenching mechanism involving electronic to vibronic energy transfer to the C–H oscillators in the hydrazine must also be considered. In 1983 Hurst and Schuster[5c] suggested that the lifetime of singlet oxygen in condensed media is limited by a similar energy-transfer exchange mechanism. The exchange energy transfer occurs by interaction between singlet oxygen and the solvent that couples the highest vibrational frequency of the solvent to an electronic transition in singlet oxygen. Schmidt and Brauer[23] demonstrated that the rate of energy transfer to a single oscillator can be expressed quantitatively by eq 12, where F_s is

$$k_{XY} = Z\sum_{sm} F_s F_m R_{sm} \qquad (12)$$

the Franck–Condon factor (FC) for the $\nu = 0 \rightarrow 1$ transition in the solvent, F_m is the FC factor for the $(^1\Delta_g, \nu = 0) \rightarrow (^3\Sigma_g, \nu = m)$ transition in oxygen, and R_{sm} is related to the off-resonance energy that must be distributed over low-energy vibrational, rotational, and translation degrees of freedom. The energy transfer becomes more efficient as the frequency of the accepting oscillator in the solvent increases, allowing increased resonant interaction with lower vibrational levels of $^3\Sigma_g(O_2)$ which have more favorable FC factors (F_m). As a result, the quenching effectiveness of various oscillators decreases in the order illustrated in Figure 5: N–H, O–H > C–H > O–D > C–D > C–Cl. Schuster[5c] and Rodgers[5b] further demonstrated that the second-order rate of singlet oxygen deactivation can be conveniently calculated by just adding up the individual contributions, k_{XY}, from all the oscillators in the solvent.

Calculations using the k_{XY} value for C–H oscillators in a methyl group reveal that the magnitude of the observed quenching rate in tetramethylhydrazine can only be explained if the efficiency of electronic-to-vibronic energy transfer were greatly enhanced by the large effective molarity of adjacent C–H bonds in a complex that forms prior to the quenching event. The very similar rates of quenching of perdeuterio- and tetramethylhydrazine, however, rule out any mechanism that relies on electronic-to-vibronic energy transfer (exclusive of the solvent bath sink) as the deactivation channel.

(19) Nelsen, S. F.; Rumack, D. T.; Meot-Ner, M. *J. Am. Chem. Soc.* **1988**, *110*, 7945.
(20) Eberson, L. In *Advances in Physical Organic Chemistry*; Academic: New York, 1982; Vol. 18, p 79.
(21) (a) Stanbury, D. M.; Haas, .; Taube, H. *Inorg. Chem.* **1980**, *19*, 518. (b) Herzberg, G. *Spectra of Diatomic Molecules*; D. Van Nostrand Co.: Princeton, NJ.
(22) Lind, J.; Shen, X.; Merényi, G.; Jonsson, B. Ö. *J. Am. Chem. Soc.* **1989**, *111*, 7654.
(23) Schmidt, R.; Brauer, H.-D. *J. Am. Chem. Soc.* **1987**, *109*, 6981.

Scheme II

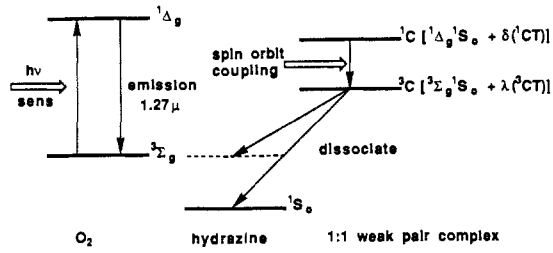

complex states are represented by product wavefunctions $^1\Delta_g$ ^1S_o and $^3\Sigma_g$ ^1S_o which are further

We believe that the most likely candidate for quenching in solution is the contact charge transfer quenching mechanism first suggested by Wilson[2a] and Ogryzlo to rationalize singlet oxygen quenching by amines.[2b] This mechanism depicted in Scheme II involves formation of a singlet charge transfer (CT) complex between $^1O_2$ and the hydrazine, intersystem crossing to a triplet CT complex, and decomposition of the triplet complex to hydrazine and $^3O_2$. The Mulliken[24] like process depicted in Scheme II occurs via three state manifolds, one for oxygen ($^3\Sigma_g$ and $^1\Delta_g$), a second for the hydrazine (^1S_o), and a third for the weak contact pair complex states ($^3C[^3\Sigma_g\,^1S_o + \lambda(^3CT)]$ and $^1C[^1\Delta_g\,^1S_o + \delta(^1CT)]$).[25] CT refers to $^{1,3}[O_2^{\bullet-}\cdots$hydrazine$^{\bullet+}]$ charge-transfer complexes with the ions in their doublet states. The complex states are represented by product wave functions $^1\Delta_g$ ^1S_o and $^3\Sigma_g$ ^1S_o that are further stabilized by some amount, δ or λ, of charge-transfer character. The process is downhill once the $^1\Delta_g$ state of oxygen is populated through the sensitizer energy-transfer process. Spin–orbit interaction will then couple the ^1C and ^3C states that then dissociate to form ground-state oxygen and hydrazine. In an elegant study, Surlock and Ogilby[26] have demonstrated, by direct irradiation of oxygen/organic molecule charge transfer complexes, that singlet oxygen is indeed coupled to the charge transfer complex state. This process requires that the ground-state 1:1 complex ^3C be less stable than either triplet oxygen or ground-state hydrazine in order to promote physical quenching.

Conclusions

These results demonstrate that hydrazines are among the most potent physical quenchers[9] of singlet oxygen known. Hydrazine **20** is more than two times more efficient at quenching $^1O_2$ in acetonitrile than strychnine, which has been touted as the fastest aliphatic tertiary amine quencher known.[27]

The quenching mechanism is best characterized as a contact charge transfer spin–orbit coupling induced process. Bimolecular outer-sphere electron-transfer reactions of hydrazines have such stringent internal reorganization requirements that they are unlikely to be observed if any other alternative mechanistic pathway is available.

Experimental Section

Preparative gas chromatographic separations were carried out on a GOW-MAC Series 550 gas chromatograph equipped with a thermal conductivity detector and a 0.25 in. × 20 ft column packed with 20% Carbowax 20M on NAW Chromosorb W 80/100. Proton and carbon NMR were obtained on a JEOL FX 270 at 269.7 and 67.8 MHz, respectively, and proton and deuterium on a JEOL GX 400 at 399.78 and 61.37 MHz, respectively. The proton and carbon spectra are referenced to TMS and the deuterium to internal $CDCl_3$.

Trimethylacetaldehyde (97%), isobutyraldehyde (99+%) gold label, dimethyl-d_6 sulfate (99+atom % D), spectrophotometric grade DMF, $LiAlH_4$, and $LiAlD_4$ were obtained from Aldrich and used without further purification. Acetonitrile, spectrophotometric grade, for kinetics, and formaldehyde were obtained from J. T. Baker, Inc. and used directly. Sodium borohydride from Ventron Alfa and Barium oxide from Barium and Chemical Inc. were also used without further purification. Tetrahydrofuran was distilled over $LiAlH_4$.

Hydrazines **1**,[28] **3**,[6] **4**,[19] **5**,[19] **6**,[6] **7**,[29] **8**,[6] **11**,[29] **14**,[6] **15**,[6] **16**,[6] **17**,[29] **18**,[6] **19**,[30] **20**,[31] **21**,[32] **22**,[6] **23**,[33] **24**,[34] and **25**[35] were synthesized with use of reported procedures. Ethyl hydrazodicarboxylate was synthesized by the method of Kauer.[36]

Tetraisobutylhydrazine (2) was prepared by reductive alkylation[28] of 1.44 g (10 mmol) of 1,2-diisobutylhydrazine with 11.52 g (160 mmol) of isobutyraldehyde and 0.912 g (24 mmol) of sodium borohydride in 50 mL of acetonitrile: bp 123–126 °C (15mm Hg), yield 0.99 g (38.7%). The product was purified for kinetic studies by preparative gas chromatography: retention time 32 min, column temperature 120 °C, injector temperature 250 °C, detector temperature 250 °C, and flow rate of He 25 mL/min. ^1H NMR ($CDCl_3$) δ 0.85 (d, J = 6.5 Hz, 24 H), 1.72 (m, 4 H), 2.08 (d, J = 6.8 Hz, 8 H).

1-Isobutyl-1,2,2-trimethylhydrazine (9) was prepared by reductive alkylation[29] of 4.8 g (41.4 mmol) of 1,1-dimethyl-2-isobutylhydrazine in 50 mL of acetonitrile with 18 g of 37% formaldehyde and 3.2 g of sodium borohydride. A 72.5% yield (3.87 g) of the product was obtained: bp 119–120 °C (580 mm Hg). Final purification prior to its kinetic examination was conducted by gas chromatography. The compound exhibited a 15 min retention time when the column temperature was 80 °C, the injector 150 °C, the detector 150 °C, and the flow rate 25 mL/min. ^1H NMR ($CDCl_3$) δ 0.90 (d, J = 7 Hz, 6 H), 1.65–1.8 (m, 1 H), 2.19 (d, J = 7 Hz, 2 H), 2.25 (s, 3 H), 2.30 (s, 6 H). ^{13}C NMR ($CDCl_3$) δ 20.8, 26.3, 35.2, 38.9, 61.7.

1,2,2-Trimethyl-1-neopentylhydrazine (10) was prepared by reductive methylation of 0.65 g (5 mmol) of 1,1-dimethyl-2-neopentylhydrazine with 3.6 g (50 mmol) of 37% formaldehyde and 380 mg (10 mmol) of sodium borohydride in 10 mL of acetonitrile. A 35% yield (0.251 g) of the product was obtained: bp 110–120 °C (580 mm Hg). The final purification prior to its kinetic study was done by preparative gas chromatography: retention time 16 min when the column temperature was 80 °C, the detector and injector temperature was 150 °C, and the flow rate was 25 mL/min. ^1H NMR ($CDCl_3$) δ 0.90 (s, 9 H), 2.23 (s, 6 H), 2.32 (s, 3 H), 2.42 (s, 2 H).

1,1-Dimethyl-2,2-dineopentylhydrazine (12) was prepared by reductive alkylation of 400 mg (3.08 mmol) of 1-neopentyl-2,2-dimethylhydrazine with 3.44 g (40 mmol) of trimethylacetaldehyde and 0.5 g of sodium borohydride in 50 mL of acetonitrile. The yield was 580 mg (62%) of 66% pure material. Final purification was conducted by preparative gas chromatography: retention time 31 min, when the column temperature was 80 °C, the injector temperature was 190 °C, the detector temperature was 230 °C, and the flow rate was 25 mL/min. ^1H NMR ($CDCl_3$) δ 0.90 (s, 18 H), 2.45 (s, 6 H), 2.55 (s, 4 H).

Ethyl 1,2-dimethyl-d_6-hydrazinedicarboxylate was prepared from 280 mg (1.9 mmol) of ethyl hydrazodicarboxylate, 353 mg (2.67 mmol) of dimethoxy sulfate-d_6, and 500 mg (3.27 mmol) of barium oxide. This mixture was stirred for 24 h at room temperature, quenched with 1 mL of H_2O, and extracted with 3 × 5 mL of ethyl ether. The ether extracts were washed with 3 × 2 mL of brine and dried by $MgSO_4$. A yield of 64% (1.21 mmol, 210 mg) was obtained after removal of ether. This material was used in the next step without further purification. ^1H NMR ($CDCl_3$) δ 1.2–1.4 (m, 6 H), 4.1–4.3 (m, 4 H). ^{13}C NMR ($CDCl_3$) δ 14.40, 14.47, 14.55, 33.42–36.15 (m), 61.90, 62.11, 62.18, 62.40, 155.43, 155.95, 156.25, 156.8. ^2H NMR (CH_3CN, internal standard $CDCl_3$) δ 2.64 (s, 6 D).

Tetramethylhydrazine-d_6 (13) was prepared by the Linke method.[28] A 1 mL THF solution of 210 mg (1.21 mmol) of ethyl 1,2-dimethyl-d_6-hydrazinedicarboxylate was added slowly to 5 mL of THF containing 100 mg (2.38 mmol) of $LiAlD_4$. The resulting mixture was refluxed for 6 h and worked up by the 1:1:3 method.[37] The precipitate was removed

(24) Tsubomura, H.; Mulliken, R. S. *J. Am. Chem. Soc.* **1960**, *82*, 5966.
(25) A reviewer has pointed out that the steric effects appear to be large for a weak contact pair complex and suggested instead that σ-bonded complexes forms. The quenching rate of the fastest hydrazine is a factor of 10 slower than diffusion control and as a result only 1 in 10 σ-bonded complexes needs to dissociate to form triplet oxygen. It is difficult to test for this mechanism, but even if it were operating at some point on the reaction surface a charge-transfer interaction to avoid the spin barrier must occur.
(26) Scurlock, R. D.; Ogilby, P. R. *J. Phys. Chem.* **1989**, *93*, 5493.
(27) Gorman, A. A.; Hamblett, I.; Smith, K.; Standen, M. C. *Tetrahedron Lett.* **1984**, 581.
(28) Linke, K.-H.; Turley, R.; Flaskamp, E. *Chem. Ber.* **1973**, *106*, 1052.
(29) Nelsen, S. F.; Weisman, G. R. *Tetrahedron Lett.* **1973**, 2321.
(30) Buhle, E. L.; Moore, A. M.; Wiselogle, F. Y. *J. Am. Chem. Soc.* **1943**, *65*, 29.
(31) Nelsen, S. F. Weisman, G. R.; Hintz, P. J.; Olp, D.; Fahey, M. R. *J. Am. Chem. Soc.* **1974**, *96*, 2916.
(32) Nelsen, S. F.; Echegoyen, L.; Clennan, E. L.; Evans, D. H.; Corrigan, D. A. *J. Am. Chem. Soc.* **1977**, *99*, 1130.
(33) Anderson, J.; Lehn, J. M. *J. Am. Chem. Soc.* **1967**, *89*, 81.
(34) Snyder, H. R., Jr.; Michels, J. G. *J. Org. Chem.* **1963**, *28*, 1144.
(35) Nelsen, S. F.; Kessel, C. R.; Brace, H. N. *J. Am. Chem. Soc.* **1979**, *101*, 1874.
(36) Kauer, J. C. *Organic Synthesis*; Wiley: New York, 1962; Collect. Vol. 4, p 411.

by suction filtration followed by addition of 2 mL of 10% HCl to convert the hydrazine to its hydrochloride salt. The THF and water were evaporated and the residue dissolved in a minimum amount of CH_3CN. After addition of powered NaOH the solution was shaken for 15 min. The hydrazine was isolated from this mixture by preparative gas chromatography with use of a column temperature of 50 °C, an injector temperature of 100 °C, a detector temperature of 150 °C, and a He flow rate of 25 mL/min. Under these conditions the hydrazine had a 13 min retention time. ^2H NMR (CH_3CN) (internal $CDCl_3$ standard) δ 1.85 (s, 12 D).

(37) Fieser, L. F.; Fieser, M. In *Reagents for Organic Synthesis*; John Wiley and Sons: New York, 1967; Vol. 1, p 584.

Acknowledgment. We thank the National Science Foundation and the donors of the Petroleum Research Foundation, administered by the American Chemical Society, for their generous support of this research. We also thank Maneesh Sharma for assistance in the synthesis of **13** and Professor S. F. Nelsen for his critical reading and useful comments on the manuscript.

Registry No. **1**, 6415-12-9; **2**, 68970-07-0; **3**, 23337-93-1; **4**, 23337-88-4; **5**, 116149-14-5; **6**, 106376-59-4; **7**, 68970-05-8; **8**, 68970-09-2; **9**, 68970-04-7; **10**, 68970-08-1; **11**, 60678-74-2; **12**, 127103-46-2; **13**, 127103-47-3; **14**, 18389-95-2; **15**, 6130-94-5; **16**, 49840-66-6; **17**, 53779-90-1; **18**, 49840-60-0; **19**, 5397-67-1; **20**, 2940-98-9; **21**, 3661-15-2; **22**, 49840-69-9; **23**, 14287-89-9; **24**, 26163-37-1; **25**, 127103-48-4; O_2, 7782-44-7.

Kinetic and Photochemical Studies of $FeC_5H_6^+$ in the Gas Phase

Yongqing Huang and Ben S. Freiser*

Contribution from the Department of Chemistry, Purdue University, West Lafayette, Indiana 47907. *Received February 21, 1989. Revised Manuscript Received September 6, 1989*

Abstract: Kinetic and photochemical studies were performed on $FeC_5H_6^+$. $FeC_5H_6^+$ was prepared by reacting Fe^+ with cyclopentene and subsequently with propane to give the cyclopentadienylallyliron ion. $D°(Fe^+–cyclopentadiene)$ was determined by photodissociation threshold measurements to be 55 ± 5 kcal/mol, which in turn indicates that dehydrogenation of cyclopentene by Fe^+ is 33 ± 5 kcal/mol exothermic. Linear kinetics are observed by collisionally cooling the $FeC_5H_6^+$ ions in a high-background pressure of argon and yield a rate constant of $5 \pm 2 \times 10^{-10}$ cm^3/(molecule·s), corresponding to a reaction efficiency of about 0.4. Photodissociation of the cyclopentadienylallyliron ion yields two product ions, $FeC_8H_8^+$ and $FeC_6H_6^+$, with the latter pathway, the higher energy process, prevailing when there is no background argon. The dehydrogenation pathway, the lower energy process, becomes more important when background argon is present to remove the excess energy from the parent ion. These results are in qualitative agreement with collision-induced dissociation experiments. Finally, $D°(CpFe^+–H) = 46 \pm 5$ kcal/mol is determined by photodissociation threshold measurements, which in turn yields $D°(Fe^+–Cp) = 88 \pm 7$ kcal/mol.

Introduction

Recently, we have begun investigating the effect of a series of ligands including alkanenitriles, arenes, and alkenes on the reactivity of gas-phase Fe^+ with propane.[1] These π-type ligands are observed not only to slow the reaction significantly but also in certain cases to open up new reaction channels. For example, at extended trapping times in a high-background pressure of propane, reactions 1–4 occur when L is an arene or alkene ligand and reactions 1–3 occur when L is an alkanenitrile ligand. In contrast, only reactions 2 and 3 are observed for bare Fe^+ with

$$FeL^+ + C_3H_8 \rightarrow FeLC_3H_8^+ \quad (1)$$

$$\rightarrow FeLC_3H_6^+ + H_2 \quad (2)$$

$$\rightarrow FeLC_2H_4^+ + CH_4 \quad (3)$$

$$\rightarrow FeLC_2H_2^+ + CH_4 + H_2 \quad (4)$$

propane.[2] During the course of this study, cyclopentadiene was observed to have a unique effect on the reaction of Fe^+ with propane. Subsequently, an in-depth study was performed on this reaction system and the results are described here.

Experimental Section

All experiments were performed on a prototype Nicolet FTMS-1000 Fourier transform mass spectrometer previously described in detail.[3] The instrument is equipped with a 5.2 cm cubic trapping cell situated between the poles of a Varian 15 in. electromagnet maintained at 0.9 T. The cell utilizes two 80% transmittance stainless steel screens as the transmitting plates, permitting the irradiation of the interior with various light sources. Fe^+ was generated by focusing the beam of a Quanta Ray Nd:YAG laser (operated at 1.064 μm) onto a thin high-purity iron target. Details of the laser ionization experiment are described elsewhere.[4]

All chemicals were obtained in high purity from commercial sources and used as supplied except for multiple freeze–pump–thaw cycles to remove noncondensible gases. Sample pressures were measured with an uncalibrated Bayard-Alpert ionization gauge. For the kinetics experiment, the propane pressure was calibrated by using a rate constant of 1.1×10^{-9} cm^3/(molecule·s) for reaction 5 and accounting for the different sensitivities of the ion gauge for propane and methane by using an experimentally determined factor of 1.8 from the literature.[5,6]

$$CH_4^+ + CH_4 \rightarrow CH_5^+ + CH_3 \quad (5)$$

Details of the collision-induced dissociation (CID) experiment have been described previously.[7] The collision energy can be varied typically in the range 0–100 eV. The spread in kinetic energy depends on the average kinetic energy and is typically about 35% at 1 eV, 10% at 10 eV, and 5% at 30 eV.[8] CID product ion distributions are reproducible conservatively to ±15% absolute.

The details of the photodissociation experiment have been described elsewhere.[9] Ions to be studied by photodissociation were first isolated

(1) Huang, Y. Ph.D. Thesis, Purdue University, 1989.
(2) (a) Halle, L. F.; Armentrout, P. B.; Beauchamp, J. L. *Organometallics* **1982**, *1*, 963. (b) Byrd, G. D.; Burnier, R. C.; Freiser, B. S. *J. Am. Chem. Soc.* **1982**, *104*, 3565. (c) Jacobson, D. B.; Freiser, B. S. *J. Am. Chem. Soc.* **1983**, *105*, 5197. (d) Schultz, R. H.; Elkind, J. L.; Armentrout, P. B. *J. Am. Chem. Soc.* **1988**, *110*, 411.
(3) Cody, R. B.; Burnier, R. C.; Freiser, B. S. *Anal. Chem.* **1982**, *54*, 96.
(4) Burnier, R. C.; Byrd, G. D.; Freiser, B. S. *J. Am. Chem. Soc.* **1981**, *103*, 4360.
(5) Huntress, W. T.; Pinizzotto, R. F. *J. Chem. Phys.* **1973**, *59*, 4742.
(6) Bartmess, J. E.; Georgiadis, R. M. *Vacuum* **1984**, *33*, 149.
(7) Jacobson, D. B.; Freiser, B. S. *J. Am. Chem. Soc.* **1983**, *105*, 736.
(8) Huntress, W. T.; Mosesman, M. M.; Elleman, D. D. *J. Chem. Phys.* **1971**, *54*, 843.
(9) Hettich, R. L.; Jackson, T. C.; Stanko, E. M.; Freiser, B. S. *J. Am. Chem. Soc.* **1986**, *108*, 5086.

0002-7863/90/1512-5085$02.50/0